Thermal effects on the photoelastic coefficient of polymer optical fibers

ACHEROY SOPHIE,[1,*] MERKEN PATRICK,[1] OTTEVAERE HEIDI,[2] GEERNAERT THOMAS,[2] THIENPONT HUGO,[2] MARQUES CARLOS A.F.,[3,4] WEBB DAVID J.,[3] GANG-DING PENG,[5] PAWEL MERGO,[6] BERGHMANS FRANCIS[2]

[1] *Dept. of Communication, Information, Systems and Sensors, Royal Military Academy, Ave Renaissance 30, 1000 Brussels, Belgium*
[2] *Vrije Universiteit Brussel (VUB), Dept. of Applied Physics and Photonics, Brussels Photonics Team (B-PHOT), Pleinlaan 2, B-1050 Brussels, Belgium*
[3] *Aston Institute of Photonic Technologies, Aston University, Aston Triangle, B4 7ET Birmingham, UK*
[4] *Instituto de Telecomunicações and University of Aveiro Physics Department & I3N, Campus de Santiago, 3810-193 Aveiro, Portugal*
[5] *Photonics & Optical Communications, School of Electrical Engineering & Telecommunications, University of New South Wales, Sydney 2052, NSW, Australia*
[6] *Laboratory of Optical Fibers Technology, Maria Curie Sklodowska University Sklodowska Sq 3, 20-031 Lublin, Poland*

**Corresponding author: sophie.acheroy@rma.ac.be*

Received XX Month XXXX; revised XX Month, XXXX; accepted XX Month XXXX; posted XX Month XXXX (Doc. ID XXXXX); published XX Month XXXX

We measure the radial profile of the photoelastic coefficient C(r) in singlemode polymer optical fibers (POFs) and we determine the evolution of C(r) after annealing the fibers at temperatures from 40°C to 80°C. We demonstrate that C(r) in the fibers drawn from a preform without specific thermal pre-treatment changes and converges to values between 1.2 to 1.6×10^{-12} Pa^{-1} following annealing at 80°C. The annealed fibers display a smoothened radial profile of C(r) and a lowered residual birefringence. In contrast, the mean value of C(r) of the fiber drawn from a preform that has been pre-annealed remains constant after our annealing process and is significantly higher, i.e 4×10^{-12} Pa^{-1}. The annealing process decreases the residual birefringence to a lower extent as well. These measurements indicate the impact of annealing on the thermal stability of the photoelastic coefficient of POFs, which is an essential characteristic in view of developing POF based thermo-mechanical sensors.

OCIS codes: *(140.3490) Lasers, distributed-feedback; (060.2420) Fibers, polarization-maintaining; (060.3735) Fiber Bragg gratings; (060.2370) Fiber optics sensors.*

http://dx.doi.org/10.1364/OL.99.099999

Polymer optical fibers (POFs) are claimed to offer an interesting alternative to glass optical fibers for sensing applications [1–3]. This essentially stems from the different material properties in terms of physical and chemical characteristics of polymers compared to glass. More specifically and for example, POFs are more flexible, they can handle larger mechanical strains, they can be processed with organic chemistry techniques and can be made biocompatible [4].

Few publications deal with the physical material characteristics, and specifically the photo-elastic properties, of POFs [5–9]. This is in contrast to silica fibers, for which these properties are relatively well documented [10–12]. The knowledge of these characteristics, along with the impact of the fabrication process on their values, is nevertheless important in view of designing and fabricating optical fibers dedicated to sensing applications. In this Letter we focus on the stress-optic coefficients C_1 and C_2 as material dependent parameters that link the change of refractive index in the fiber caused by an external load, and more particularly on the photoelastic constant $C = C_1 - C_2$. Our research has been prompted by [13], which reported that annealing of POFs partially relieves frozen-in stresses induced by the fiber drawing process, and which results in an increase of the sensitivity to stress and strain of the fiber. Additionally, reference [14] reports that annealing the fiber reduces the cross-sensitivity of POF based sensors to both temperature and strain variations.

We have recently developed a method to determine the stress-optic constant C and its radial distribution in the fiber cross-section, with the measurement method and algorithm detailed in previous publications [15–17]. The main steps of our method are briefly recalled here for the sake of completeness. We illuminate the optical fiber transversally (along the x-axis) with monochromatic light at 633 nm, polarized at 45° with respect to the fiber axis. The

wave vector is perpendicular to the fiber axis taken along the z-axis. Additionally the fiber is immersed in index matching liquid to avoid refraction phenomena at the fiber-air boundaries. During illumination we apply a known axial load inducing a normal stress σ_z which is assumed to be constant over the fiber cross section. In its turn the normal stress induces birefringence in the fiber, which causes a phase-shift between the two linear polarized components of the illumination. This is observed as a projected retardance R(y) following propagation through the fiber, where y is the other transversal coordinate. R(y) is related to the normal stress by means of the inverse Abel transform [18].

$$\sigma_z \times \mathrm{C}(r) = -\frac{1}{\pi}\int_r^b \frac{dR(y)/dy}{\sqrt{y^2 - r^2}}\,dy \qquad \textbf{(1)}$$

We can derive the photoelastic constant from equation (1). It is the regression coefficient C(r) linking the inverse Abel transform of R(y) and the known axial stress σ_z. r is the radial distance from the center of the fiber and b is the radius of the fiber.

We measure R(y) using the Sénarmont compensation method. We use a polarizing microscope to achieve a full-field view of the retardance. The algorithm to calculate the inverse Abel transform of R(y) is based on Fourier theory and is extensively described in [15,16] along with the discussion of measurement results on glass optical fibers.

Note that the mean value of C can also be determined. If one assumes that σ_z and C are constant over the fiber cross-section, the shape of R(y) can be approximated with a semi-ellipse E(y). The inverse Abel transform of E(y) is constant and depends solely on the semi-short and the semi-long axes of the ellipse. The expression between the axial stress and the retardance then becomes:

$$\sigma_z \times C + K_0 = -\frac{1}{2}\frac{a}{b} \qquad \textbf{(2)}$$

where b is the fiber radius, and a = max(abs(R(y))), σ_z the axial stress and K_0 a constant defined by the inverse Abel transform of the retardance caused by the residual birefringence of the fiber when it is not submitted to an external load. Again, C is the regression coefficient that has to be determined. The elliptical approximation therefore also allows estimation of the residual birefringence in the fiber, assuming that K_0 is constant over the fiber cross-section.

Using the technique explained above, we determine C(r) in samples of three similar single mode step-index polymer optical fibers, labeled Fiber 1 to Fiber 3, drawn in the same facility with similar drawing conditions [19–21]. The draw tension for all 3 fibers was below 1N. The core and cladding dimensions of the fibers are respectively 10µm/110µm, 10µm/133µm and 12µm/260µm. The core of the fibers is composed of poly-ethyl methacrylate and poly-benzyl methacrylate (PEMA/PBzMA) [22], whilst the cladding is made of poly-methyl methacrylate (PMMA). Variations in drawing conditions can for example lead to core/cladding ratio differences resulting from fluctuating fluid dynamic responses of the two polymers (PMMA and PEMA/PBzMA), yet the largest part of the fiber consists of PMMA considering the small dimensions of the core. Fiber 1 and Fiber 2 are fabricated from the same preform, whilst fiber 3 was obtained from a second preform. The preforms were obtained following thermal curing of the polymer. For the first preform the temperature was increased from 45°C to 75°C within 4 days. The second preform was obtained after heating from 36°C to 88°C within 4.5 days until solidification. The preforms were then heat-drawn into optical fibers at respectively 220°C and 225°C.

We first determine both the mean value of C and C(r) for the pristine samples. We then anneal the samples for 8 hours at respectively 40°C, 60°C and 80°C and we determine the mean value of C and C(r) following each annealing step. PMMA based POFs are well known to be sensitive to humidity [23–25]. Whilst we could not control the history in terms of exposure to environmental temperature and humidity changes between their fabrication and arrival in our laboratories, we emphasize that we in between the annealing steps carried out in our labs, all fiber samples were stored and measured in the same temperature (20°C) and relative humidity (50%) controlled cleanroom and therefore in the same environmental conditions. To ensure that the fibers were uniform along their length, we have carried out measurements on several fiber portions taken from a single fiber length. We obtained similar results in terms of value of C (not shown here for the sake of conciseness), which confirms the axial uniformity of the measured fibers.

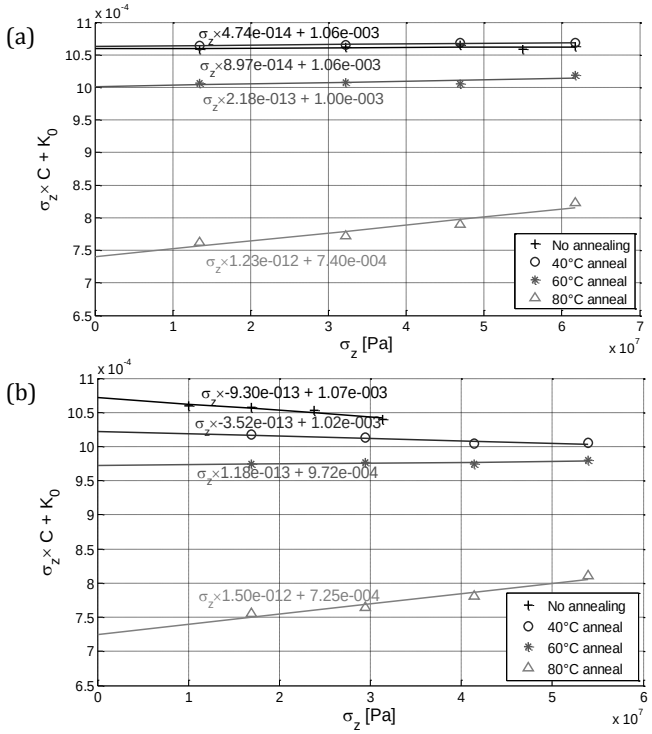

Fig. 1. σz×C + K0 as a function of the axial stress measured on a sample of (a) Fiber 1 and (b) Fiber 2. The regression coefficient is the mean photoelastic constant C. The values of C and the extrapolated values of the residual stress are indicated in the graph along the respective linear fits.

Fig. 1 illustrates the results obtained for Fiber 1 and Fiber 2. Similar graphs are obtained for Fiber 3. The constant K_0 of the fiber clearly decreases with increasing annealing temperatures, indicating the decrease of the residual birefringence and hence of the residual stress in these samples. K_0 in the samples annealed at 80°C is 36% lower for Fiber 1 and Fiber 2, and 17% lower for Fiber 3 compared to the pristine samples.

Table 1: Measured stress-optic coefficient and K_0 for fibers for different annealing temperature.

	Temp	Fiber 1	Fiber 2	Fiber 3	Fiber 4	Fiber 5
Diameter [µm]		110	133	260	110	210
Draw Tension D_T		<< 1N	<< 1N	<<1N	*	0,5 < D_T < 1N
Draw ratio [mm]		16/0,11	16/0,133	16/0,26	*	11/0,21
C $\times 10^{-12}$ Pa^{-1}	No	0,047	-0,93	0,504	-0,15	3,85
	40°C	0,089	-0,35	0,75	-0,124	4,08
	60°C	0,218	0,118	1,06	-0,099	3,83
	80°C	1,23	1,50	1,57	1,54	3,94
K_0 [$\times 10^{-4}$]	No	11	11	5,9	10	2,3
	40°C	11	10	5,9	9	2,3
	60°C	10	10	5,6	8	2,3
	80°C	7,4	7,2	4,8	6	2,1

* The draw tension and draw ratio for fiber 4 have not been communicated by the manufacturer.

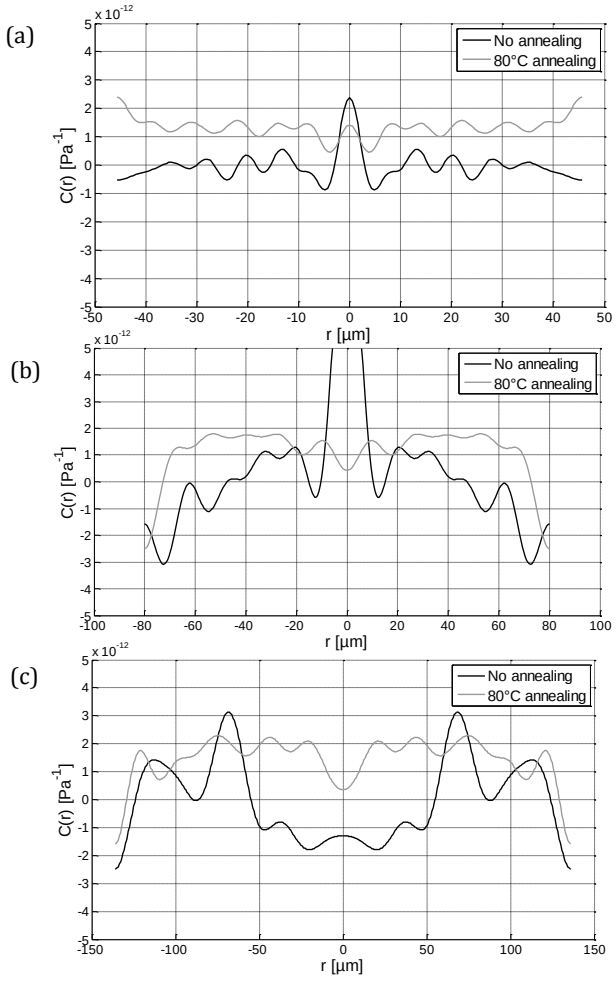

Fig. 2. Comparison of the radial distribution of the photoelastic coefficient C(r) of the POFs under test without annealing and with 8 hours annealing at 80°C in Fiber 1, (b) Fiber 2 and (c) Fiber 3.

The mean value of the stress-optic coefficient tends to reach comparable values between 1.2×10^{-12} Pa^{-1} to 1.6×10^{-12} Pa^{-1} for the three fibers. Fig. 1 illustrates the results obtained for Fiber 1 and Fiber 2. Similar graphs are obtained for Fiber 3. The constant K_0 of the fiber clearly decreases with increasing annealing temperatures, indicating the decrease of the residual birefringence and hence of the residual stress in these samples. K_0 in the samples annealed at 80°C is 36% lower for Fiber 1 and Fiber 2, and 17% lower for Fiber 3 compared to the pristine samples.

Table 1 summarizes the values of C and the constant K_0 we measured on the three fibers for increasing annealing temperature.

The radial profile C(r) of the pristine fiber samples and these of the samples annealed at 40°C and 60°C are comparable. After annealing at 80°C however, the effect of the higher temperature is clearly visible. Therefore and for the sake of clarity we only compare the C(r) profiles before annealing and after annealing at 80°C in Fig. 2. This annealing process increases the value of the mean stress-optic constant. The variance of the measurements of fiber 2 without annealing is slightly higher than that of fiber 1. This has a direct impact on the calculation and result of the inverse Abel transform of the retardance. Our results nevertheless clearly show the effect of annealing the POFs at a higher temperature. The variance decreases in both fibers, which explains a smoother and more constant C(r) profile throughout the fiber cross-section. Note that the overshoot at r = 0, i.e. in the center of the fiber, stems from a numerical artefact of the inverse Abel transform. The height of the overshoot depends on the amount of Fourier coefficients considered in the expansion of the inverse Abel transform, as we explained in details in [15], and cannot be related to an actual property of the optical fiber.

To substantiate our findings, we repeated the same measurements on two other types of single mode polymer fibers (Fiber 4 and Fiber 5). Fiber 4 has a PMMA core doped with 5% polystyrene, and a cladding composed of pure PMMA [26,27]. Fiber 5 also has a PMMA cladding and a core composed of PMMA doped with 2,4,6-trichlorophenil methacrylate. The preform of Fiber 5 was annealed for 2 weeks at 80°C before the fiber was heat-drawn at 290°C with a draw tension below 1N. The core/cladding dimensions of these two fibers are respectively 9µm/110µm and 4µm/210µm.

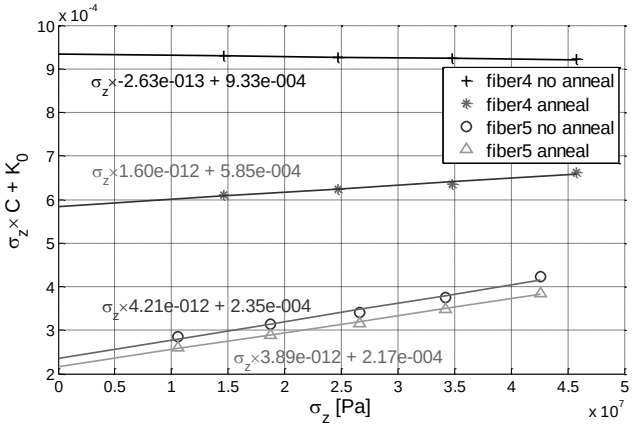

Fig. 3. $\sigma_z \times C + K_0$ as a function of the axial stress measured on a sample of Fiber 4 and Fiber 5. The values of C and the extrapolated values of the residual stress are indicated in the graph along the respective linear fits.

Fig. 3 shows the mean value of C. The impact of annealing on Fiber 4 is comparable to that on Fibers 1 to 3. K_0 decreases significantly, whilst the mean value of C increases from $-2{,}63\times10^{-13}$ Pa^{-1} to $1{,}60\times10^{-12}$ Pa^{-1}. In Fiber 5, for which the preform has been annealed prior to drawing, the decrease of K_0 is less pronounced

(7,7%), but the mean value of C also remains almost constant. Fig. 4 shows the radial profile of the stress-optic constant for both fibers measured before and after annealing at 80°C. The evolution of the radial profile of C(r) for Fiber 4 is comparable to our previous findings. The radial profile of C(r) of Fiber 5, however, is not at all affected by the annealing process. Recall that the preform of this fiber has been annealed for 2 weeks at 80°C. Note also that for Fiber 5, we find a value of C of 4×10^{-12} Pa^{-1}, which is larger than the values measured for Fibers 1 to 4.

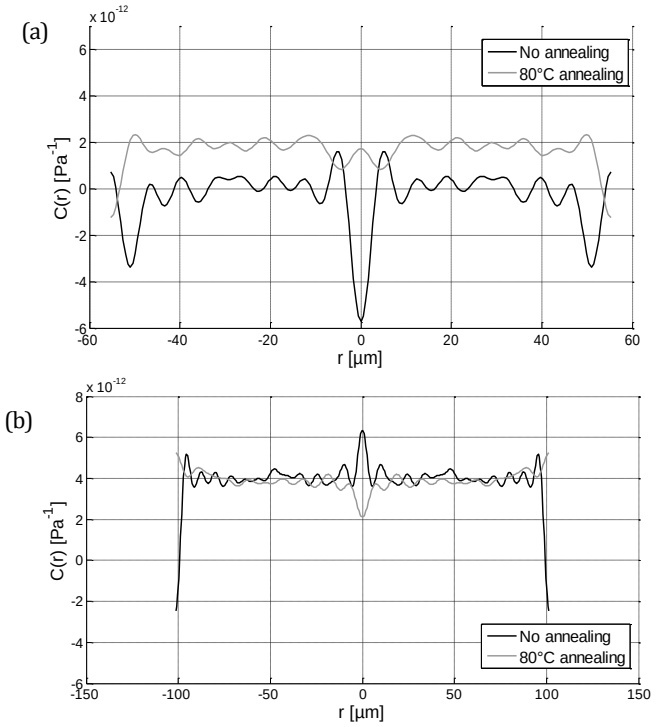

Fig. 4. Comparison of the radial distribution of the photoelastic coefficient C(r) of (a) Fiber 4 and (b) Fiber 5 before and after 8 hours annealing at 80°C.

To conclude, we have determined the radial profile of the photoelastic constant C(r) and its mean value in 5 different polymer optical fibers. We have also analyzed the effect of annealing on that material parameter and we quantified the impact of annealing on the residual stress in the POF. Annealing at 40°C and 60°C did not significantly affect C(r) and K_0 for any of the fiber samples. Annealing at a higher temperature, i.e. 80°C, of fibers drawn from a preform without any specific annealing treatment did impact both parameters. The radial profile of C(r) is more regular and clean, which may indicate a reduced variation of the material parameter C throughout the fiber section and an increased homogeneity in the cross-section of the POF. Additionally, annealing increases significantly the mean value of C(r) but decreases the residual birefringence throughout the fiber section. This may explain the findings reported in [14] i.e. the higher sensitivity to stress and strain but a lower cross-sensitivity to strain and temperature, respectively of the annealed fiber.

The effect of annealing on a POF of which the preform has been annealed prior to drawing is different. This fiber is much less sensitive to thermal treatment as shown with Fiber 5.

In future work, we will address the actual influence of annealing on the strain sensitivity of the fiber.

Acknowledgment. This work was partially supported by the IWT-SBO Project with Contract 120024 'Self Sensing Composites - SSC'. T. Geernaert is post-doctoral research fellow with the Research Foundation Flanders (FWO). The authors would also like to acknowledge financial support from the Methusalem and Hercules Foundations. The Belgian Science Policy Interuniversity Attraction Pole P7/35 is acknowledged as well. Carlos A.F. Marques was supported by Marie Curie Intra European Fellowship included in the 7th Framework Program of the European Union (project PIEF-GA-2013-628604) and FCT Fellowship (SFRH/BPD/109458/2015).

References

1. K. Peeters, Smart Mater. Struct. **20**, (2011).
2. N. G. Harbach, **4021**, 118 (2008).
3. F. Berghmans and H. Thienpont, OFC 3 (2014).
4. D. J. Webb, Meas. Sci. Technol. **26**, 092004 (2015).
5. A. Tagaya, T. Harade, K. Koike, and Y. Koike, J. Appl. Polym. Sci. **106**, 4219 (2007).
6. A. Tagaya, L. Lou, Y. Ide, Y. Koike, and Y. Okamoto, Sci. China Chem. **55**, 850 (2012).
7. R. M. Waxler, D. Horowitz, and A. Feldman, Appl. Opt. **18**, 101 (1979).
8. H. Ohkita, K. Ishibashi, D. Tsurumoto, A. Tagaya, and Y. Koike, Appl. Phys. A **81**, 617 (2005).
9. F. Ay, A. Kocabas, C. Kocabas, A. Aydinli, and S. Agan, J. Appl. Phys. **96**, 7147 (2004).
10. W. Primak, J. Appl. Phys. **30**, 779 (1959).
11. N. Lagakos and R. Mohr, Appl. Opt. **20**, 2309 (1981).
12. A. Bertholds and B. Dändliker, J. Light. Technol. **6**, 17 (1988).
13. W. Yuan, A. Stefani, M. Bache, T. Jacobsen, B. Rose, N. Herholdt-Rasmussen, F. K. Nielsen, S. Andresen, O. B. Sørensen, K. S. Hansen, and O. Bang, Opt. Commun. **284**, 176 (2011).
14. R. Oliveira, C. A. F. Marques, L. Bilro, and R. N. Nogueira, 23rd Int. Conf. Opt. Fibre Sensors **9157**, 9 (2014).
15. S. Acheroy, P. Merken, H. Ottevaere, T. Geernaert, H. Thienpont, and F. Berghmans, Appl. Opt. **52**, 8451(2013).
16. S. Acheroy, P. Merken, T. Geernaert, H. Ottevaere, H. Thienpont, and F. Berghmans, Opt. Express **23**, 18943 (2015).
17. S. Acheroy, M. Patrick, G. Thomas, H. Ottevaere, H. Thienpont, and F. Berghmans, in Optical Sensing and Detection III, F. Berghmans, A. G. Mignani, and P. De Moor, eds. (Proc. of SPIE Vol. 9141, 914115, 2014).
18. P. L. Chu and T. Whitbread, Appl. Opt. **21**, 4241 (1982).
19. H. Y. Liu, G. D. Peng, and P. L. Chu, IEEE Photonics Technol. Lett. **14**, 935 (2002).
20. Y. Luo, B. Yan, M. Li, X. Zhang, W. Wu, Q. Zhang, and G.-D. Peng, Opt. Fiber Technol. **17**, 201 (2011).
21. W. Wu, Y. Luo, X. Cheng, X. Tian, W. Qiu, B. Zhu, G. Peng, and Q. Zhang, **12**, 1652 (2010).
22. H. Y. Liu, G. D. Peng, and P. L. Chu, IEEE Photonics Technol. Lett. **13**, 824– (2001).
23. G. Woyessa, A. Fasano, A. Stefani, C. Markos, K. Nielsen, H. K. Rasmussen, and O. Bang, Opt. Express **24**, 1253 (2016).
24. G. Woyessa, K. Nielsen, A. Stefani, C. Markos, and O. Bang, Opt. Express **46**, 643 (2011).
25. P. Stajanca, O. Cetinkaya, M. Schukar, P. Mergo, D. J. Webb, and K. Krebber, Opt. Fiber Technol. **28**, 11 (2016).
26. "http://www.paradigmoptics.com/," .
27. C. A. F. Marques, L. B. Birlo, N. J. Alberto, D. J. Webb, and R. N. Nogueira, Opt. Commun. **307**, 57 (2013).

1. K. Peeters, "Polymer optical fibre sensors - A review," Smart Mater. Struct. **20**, (2011).
2. N. G. Harbach, "Fiber bragg gratings in Polymer Optical Fibers," **4021**, 118 (2008).
3. F. Berghmans and H. Thienpont, "Plastic Optical Fibers for Sensing Applications," OFC 3–5 (2014).
4. D. J. Webb, "Fibre Bragg grating sensors in polymer optical fibres," Meas. Sci. Technol. **26**, 092004 (2015).
5. A. Tagaya, T. Harade, K. Koike, and Y. Koike, "Improvement of the physical properties of poly(methyl methacrylate) by copolymerization with pentafluorophenyl methacrylate," J. Appl. Polym. Sci. **106**, 4219–4224 (2007).
6. A. Tagaya, L. Lou, Y. Ide, Y. Koike, and Y. Okamoto, "Improvement of the physical properties of poly(methyl methacrylate) by copolymerization with N-pentafluorophenyl maleimide; zero-orientational and photoelastic birefringence polymers with high glass transition temperatures," Sci. China Chem. **55**, 850–853 (2012).
7. R. M. Waxler, D. Horowitz, and A. Feldman, "Optical and physical parameters of Plexiglas 55 and Lexan," Appl. Opt. **18**, 101–104 (1979).
8. H. Ohkita, K. Ishibashi, D. Tsurumoto, A. Tagaya, and Y. Koike, "Compensation of the photoelastic birefringence of a polymer by doping with an anisotropic molecule," Appl. Phys. A **81**, 617–620 (2005).
9. F. Ay, A. Kocabas, C. Kocabas, A. Aydinli, and S. Agan, "Prism coupling technique investigation of elasto-optical properties of thin polymer films," J. Appl. Phys. **96**, 7147–7153 (2004).
10. W. Primak, "Photoelastic constants of vitreous Silica and its elastic coefficient of refractive index," J. Appl. Phys. **30**, 779–788 (1959).
11. N. Lagakos and R. Mohr, "Stress optic coefficient and stress profile in optical fibers," Appl. Opt. **20**, 2309–2313 (1981).
12. A. Bertholds and B. Dändliker, "Determination of the individual strain-optic coefficients in single-mode optical fibers," J. Light. Technol. **6**, 17–20 (1988).
13. W. Yuan, A. Stefani, M. Bache, T. Jacobsen, B. Rose, N. Herholdt-Rasmussen, F. K. Nielsen, S. Andresen, O. B. Sørensen, K. S. Hansen, and O. Bang, "Improved thermal and strain performance of annealed polymer optical fiber Bragg gratings," Opt. Commun. **284**, 176–182 (2011).
14. R. Oliveira, C. A. F. Marques, L. Bilro, and R. N. Nogueira, "Production and characterization of Bragg gratings in polymer optical fibers for sensors and optical communications," 23rd Int. Conf. Opt. Fibre Sensors **9157**, 9–12 (2014).
15. S. Acheroy, P. Merken, H. Ottevaere, T. Geernaert, H. Thienpont, and F. Berghmans, "Influence of measurement noise on the determination of the radial profile of the photoelastic coefficient in step-index optical fibers.," Appl. Opt. **52**, 8451–9 (2013).
16. S. Acheroy, P. Merken, T. Geernaert, H. Ottevaere, H. Thienpont, and F. Berghmans, "Algorithms for determining the radial profile of the photoelastic coefficient in glass and polymer optical fibers," Opt. Express **23**, 18943 (2015).
17. S. Acheroy, M. Patrick, G. Thomas, H. Ottevaere, H. Thienpont, and F. Berghmans, "On a possible method to measure the radial profile of the photoelastic constant in step-index optical fiber," in *Optical Sensing and Detection III*, F. Berghmans, A. G. Mignani, and P. De Moor, eds. (Proc. of SPIE Vol. 9141, 914115, 2014).
18. P. L. Chu and T. Whitbread, "Measurement of stresses in optical fiber and preform," Appl. Opt. **21**, 4241–4245 (1982).
19. H. Y. Liu, G. D. Peng, and P. L. Chu, "Polymer fiber Bragg gratings with 28-dB Transmission Rejection," IEEE Photonics Technol. Lett. **14**, 935–937 (2002).
20. Y. Luo, B. Yan, M. Li, X. Zhang, W. Wu, Q. Zhang, and G.-D. Peng, "Analysis of multimode POF gratings in stress and strain sensing applications," Opt. Fiber Technol. **17**, 201–209 (2011).
21. W. Wu, Y. Luo, X. Cheng, X. Tian, W. Qiu, B. Zhu, G. Peng, and Q. Zhang, "Design and fabrication of single mode polymer optical fiber gratings," **12**, 1652–1659 (2010).
22. H. Y. Liu, G. D. Peng, and P. L. Chu, "Thermal tuning of polymer optical fiber Bragg gratings," IEEE Photonics Technol. Lett. **13**, 824–826 (2001).
23. G. Woyessa, A. Fasano, A. Stefani, C. Markos, K. Nielsen, H. K. Rasmussen, and O. Bang, "Single mode step-index polymer optical fiber for humidity insensitive high temperature fiber Bragg grating sensors," Opt. Express **24**, 1253 (2016).
24. G. Woyessa, K. Nielsen, A. Stefani, C. Markos, and O. Bang, "Temperature insensitive hysteresis free highly sensitive polymer optical fiber Bragg grating humidity sensor," Opt. Express **46**, 643–644 (2011).
25. P. Stajanca, O. Cetinkaya, M. Schukar, P. Mergo, D. J. Webb, and K. Krebber, "Molecular alignment relaxation in polymer optical fibers for sensing applications," Opt. Fiber Technol. **28**, 11–17 (2016).
26. "http://www.paradigmoptics.com/," .
27. C. A. F. Marques, L. B. Birlo, N. J. Alberto, D. J. Webb, and R. N. Nogueira, "Narrow bandwidth Bragg gratings imprinted in polymer optical fibers for different spectral windows," Opt. Commun. **307**, 57–61 (2013).